Progress In Electromagnetics Research, PIER 38, 147–166, 2002

COMPARATIVE ANALYSIS BETWEEN CONICAL AND GAUSSIAN PROFILED HORN ANTENNAS

A. A. Kishk and C.-S. Lim

Department of Electrical Engineering
The University of Mississippi
University, MS 38677, USA

Abstract—A parametric study is performed to the conical and Gaussian profiled horn antennas. Corrugations are added to these horns to further improve their radiation characteristics. The analyses are performed numerically using a body of revolution code, which uses the method of moments. The obtained numerical results are illustrated graphically to show the performance of the horns in terms of phase center, return loss, efficiency with parabolic reflector, directivity, and cross polarization of the horns. Results obtained conclude that the Gaussian profiled horns perform better than the existing conical horn antenna system. The Gaussian profiled horns provide higher efficiency, lower cross polarization, lower sidelobe levels as well as wider bandwidth. The objective of this article is to provide some understanding to the Gaussian profiled horns that might be of help to the new antenna designers.

1. INTRODUCTION

We are not going to provide a long introduction to the subject matter because the literature is full of many references that the reader can find in [1–3]. Aperture antennas are commonly used with satellite systems. As one of the aperture antennas horn antennas are widely used as a direct radiator or as a feed for the parabolic reflectors. Normally, the horn antenna consists of an aperture, which is connected to the waveguide through a flared region, which provides a smooth transition between the waveguide and free space. The corrugated conical horn antenna with excitation from a circular waveguide is commonly used to produce high radiation efficiency. As a feed for reflector antenna, the performance of the feed has significant effect on the performance of the whole reflector system. To improve the antenna efficiency, the Gaussian profiled horn antenna [4, 5] is introduced. The Gaussian profiled horn antenna provides a smoother transition from the waveguide to the aperture improving the matching between the antenna and free space [6]. This better matching provides better radiation pattern plus wider bandwidth and perhaps more importantly, has more than 80% reflector efficiency.

In this paper, two different horns, the Gaussian profiled and conical horn, will be studied. Two different Gaussian profiles are examined. The objective of the paper is to understand the discrete importance of the horn parameters to the horn performance. We will compare the performance of the horns in terms of the phase center, return loss, efficiency with parabolic reflector, directivity, and cross polarization of the horn.

2. STUDIED PROFILE

The conical horn can be described in terms of the radial radii from the horn axis of symmetry (z-axis) as

$$\rho(z) = a_w + \frac{(\rho_0 - a_w)(z + L)}{L} \tag{1}$$

where a_w is the waveguide radius, ρ_0 is the horn aperture radius, and L is the horn length from the waveguide opening to the horn aperture as shown in Fig. 1. The Gaussian horn profiles are described in two forms. The first form is described by the radial variations as a function of the axial distance z from the waveguide opening as [7]

$$\rho(z) = \begin{cases} g(z + L) & z < -L/2 \\ 2g(L/2) - g(z) & z \geq -L/2 \end{cases} \tag{2}$$

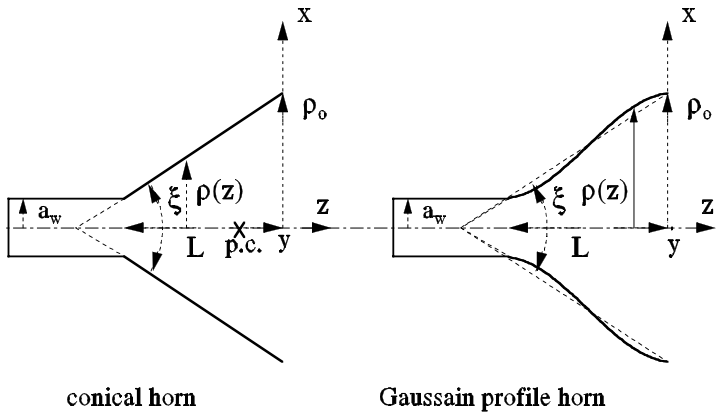

Figure 1. Coordinate system and the parameters of the conical and Gaussian profiled horn antennas.

where

$$g(\zeta) = a_w \sqrt{1 + \left(\frac{\zeta}{\alpha k a_w^2}\right)^2} \tag{3}$$

This profile is referred to as **Profile 1** in this paper. It depicts the super impose of two hyperbolas, one concave and the other convex. The variable **k** in the equation is the propagation constant. The value of α controls the horn antenna slope. Consequently, this also determines the aperture radius. During the simulation, the variable **L** and a_w are fixed. The aperture radius is then computed by the given equation. The second profile is defined as [8].

$$\rho(z) = a_w + (\rho_0 - a_w)\left\{\frac{(1-A)(z+L)}{L} + A\sin^2\left(\frac{\pi[z+L]}{2L}\right)\right\} \tag{4}$$

This profile is referred to as **Profile 2**. **Profile 1** is different from **Profile 2** in terms of its curvature. While **Profile 1** has a fixed curvature, **Profile 2**'s curvature is variable. The variable **A** in the above expression determines the curvature of the monomode Gaussian profiled antenna. The curvature increases when the value of **A** increases. We vary the radius of the outer operture with **L**, **A**, and a_w are fixed.

3. COMPUTATION

The analysis is performed numerically using a code based on the method of moments for bodies of revolution [9]. This code has been

tested and used in the design of many antennas. The results obtained by this code are very reliable and accurate. The code provides different characteristics of the horn such as, radiation pattern, directivity, return loss, and analysis of the horn performance with the proper parabolic reflector antenna as a prime focus feed.

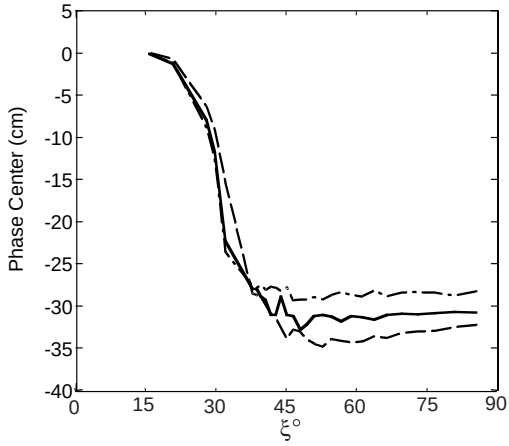

Figure 2. Phase center from the aperture of the horn versus the apex angle (---- Conical, —— profile 1 Gaussian, and $-\cdot-$ profile 2 Gaussian).

4. SMOOTH-WALLED CONICAL AND GAUSSIAN PROFILED HORNS

The smooth-walled conical horn and the Gaussian profiled horns are analyzed as feeds for the parabolic reflector antenna. The results of these horns are compared with each other graphically. We tried to use parameters that are common between them for a fair comparison between these antennas. Here, we choose the following parameters: $\mathbf{L} = 8\lambda$, $a_w = 0.4\lambda$, $\mathbf{A} = 0.8$ at an operating frequency of 8 GHz. The variable α and ρ_0 are varied as the horn aperture radius changes. First the phase center location (p.c.) from the horn aperture is plotted in Fig. 2. It can be seen that the phase center is located at the horn aperture when the flare angle (apex angle) is very close. As the apex angle increases, the phase center moves rapidly toward the waveguide opening. When the apex angle exceeds 45° the phase center remains very close to the waveguide aperture. In the case of the conical horn, the phase center moved inside the waveguide aperture by a very small distance. The Gaussian profile horns have almost

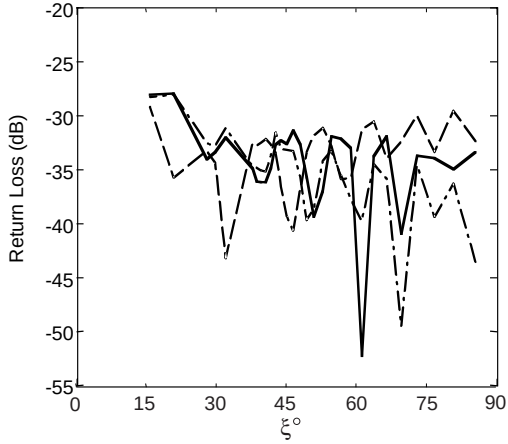

Figure 3. Return loss versus the horn apex angle (---- Conical, —— profile 1 Gaussian, and $-\cdot-$ profile 2 Gaussian).

constant phase center location as the apex angle increases. Fig. 3 shows the return loss of these horns as the apex angle increases. All horns show very good return loss level, but the conical horn shows a higher average return loss and the return loss average increases as the apex angle increases more than 45°. Figs. 4a and 4b show the maximum efficiency of the reflector antenna using these feeds and the corresponding suspended reflector aperture angle, respectively. It can be seen that with a small horn apex angle the conical horn gives higher efficiency, but with a larger apex angle, the efficiency is smaller than those obtained from the Gaussian profiled horns. The corresponding reflector suspended angle is almost the same for all horns. One correlation could be mentioned here, the efficiency of the reflector has its minimum where the phase center location is varying rapidly. Figs. 5a and 5b show the 10 dB half beamwidth of the E-plane and H-plane, respectively. These figures show that the radiation patterns of all horns are not symmetry (equal E- and H-plane), but the average value between the E-plane and H-plane 10 dB beamwidth is corresponding to the reflector suspended angle at which maximum efficiency can be obtained. Also, the maximum cross-polarization levels are computed in the 45° azimuthal plane according to Ludwig third definition [10] as shown in Fig. 6a. Fig. 6b shows the angle at which the maximum cross-polarization occurs. This is very important, because if the maximum cross polarization level is not acceptable and occurs within the 10 dB beamwidth, the secondary radiation pattern of the reflector antenna might be deteriorated. The maximum cross-

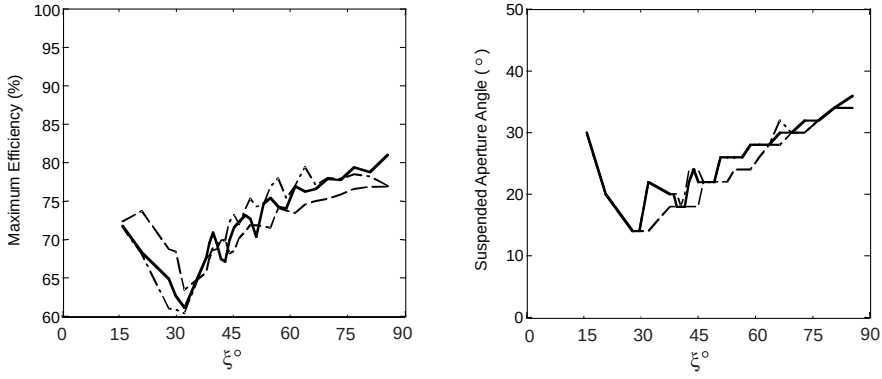

(a) (b)

Figure 4. Maximum reflector efficiency, (a) and the corresponding suspended angle, (b), versus the horn apex angle (---- Conical, —— profile 1 Gaussian, and —·— profile 2 Gaussian).

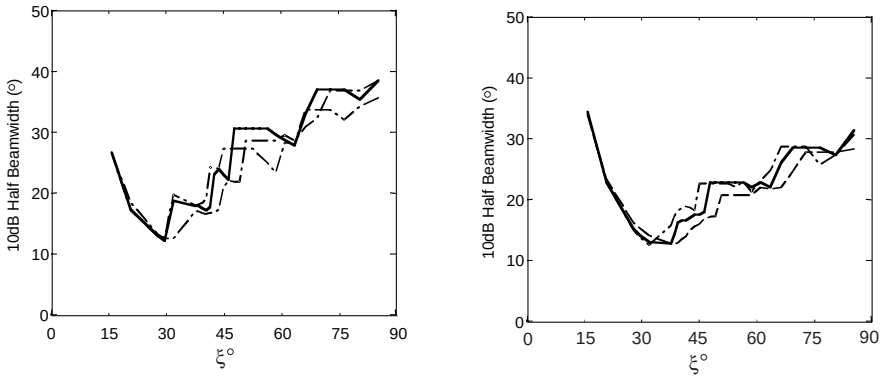

(a) (b)

Figure 5. 10 dB half beamwidth versus the horn apex angle, (a) E-plane, (b) and H-plane (---- Conical, —— profile 1 Gaussian, and —·— profile 2 Gaussian).

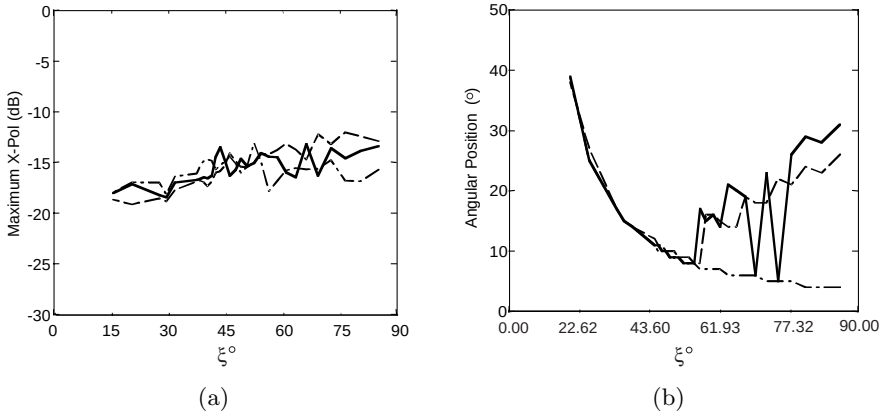

Figure 6. Maximum cross polarization and its elevation position versus the horn apex angle (---- Conical, —— profile 1 Gaussian, and −·− profile 2 Gaussian).

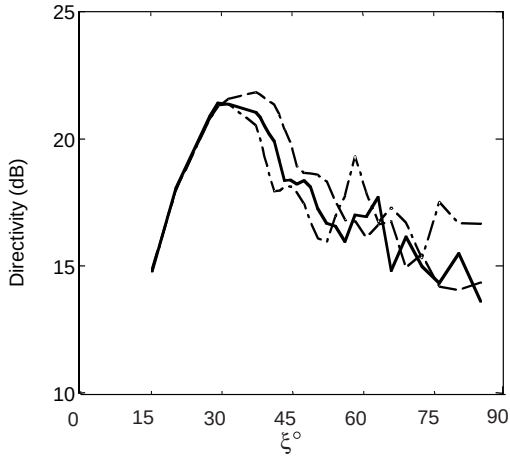

Figure 7. Directivity of the horn versus its apex angle (---- Conical, —— profile 1 Gaussian, and −·− profile 2 Gaussian).

polarization level is between −12 and −20 dB for all horns. The directivity of the horns are computed and plotted in Fig. 7. The maximum directivity is achieved by the conical horn when the apex angle is about 40°.

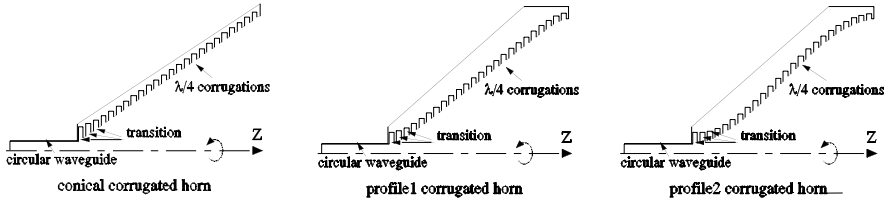

(a) (b) (c)

Figure 8. Cross-section geometry of the corrugated horns.

5. CORRUGATED CONICAL AND GAUSSIAN PROFILED HORNS

To improve the radiation characteristics of the horn antennas, corrugations are added to the horn antenna for a dual mode horn feed. The TM_{11} mode is generated internally, in addition to the dominant TE_{11} mode of the circular waveguide, to alter the TE_{11} mode field distribution in the E-plane to be nearly like that in the H-plane. The antenna started with a monomode smooth circular waveguide to generate a TE_{11} mode. A surface impedance adapter, from $\lambda/2$ to $\lambda/4$ depth corrugation is applied to the first three corrugations close to the waveguide opening [7] as shown in Fig. 8. At the output of the aperture, a combination of TE_{11} and TM_{11} mode, described as the hybrid HE_{11} mode, is produced. Using the same value of parameters as before ($\mathbf{L} = 8\lambda$, $a_w = 0.4\lambda$, $\mathbf{A} = 0.8$ at 8 GHz), the results in Fig. 9 to 14 are obtained. These results correspond to the results in Fig. 2 to 7, respectively. Generally, one can notice the similarity in the performance of the smooth wall and corrugated wall horns. The corrugated horns show better performance in terms of the cross-polarization level, symmetry of the radiation patterns, lower return loss, and higher reflector aperture efficiency.

As expected, the corrugated antennas produce lower cross polarization levels, more symmetrical E-plane and H-plane, better radiation pattern and higher maximum efficiency compared to smooth-walled horns. Fig. 9 shows that the phase center location of the Gaussian profiled horn keeps nearly unchanged despite increasing the aperture size of the horn. The constant phase center indicates that the aperture phase error is very small compared to the conical horn. The smooth transition between the waveguide and the aperture reduces the return loss of the Gaussian profiled horn when the apex angle increases ($> 45°$). In retrospect, the sudden transition for a conical horn between the waveguide and the aperture in the case of a conical horn causes it to have a higher return loss although the impedance transformer exist

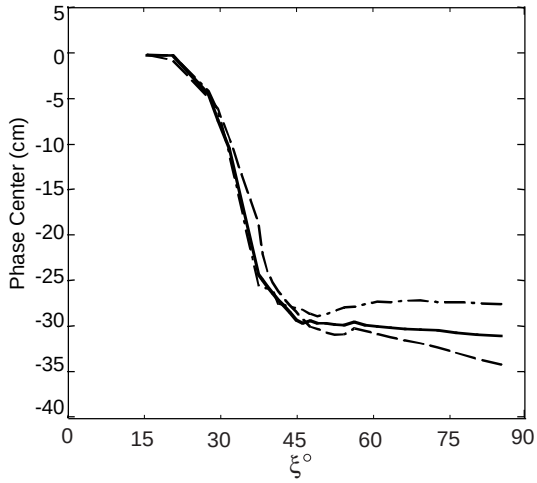

Figure 9. Phase center from the aperture of the horn versus the apex angle (---- Conical, —— profile 1 Gaussian, and —·— profile 2 Gaussian).

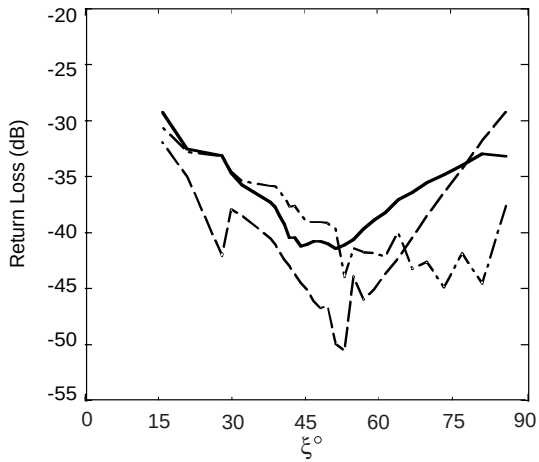

Figure 10. Return loss versus the horn apex angle (---- Conical, —— profile 1 Gaussian, and —·— profile 2 Gaussian).

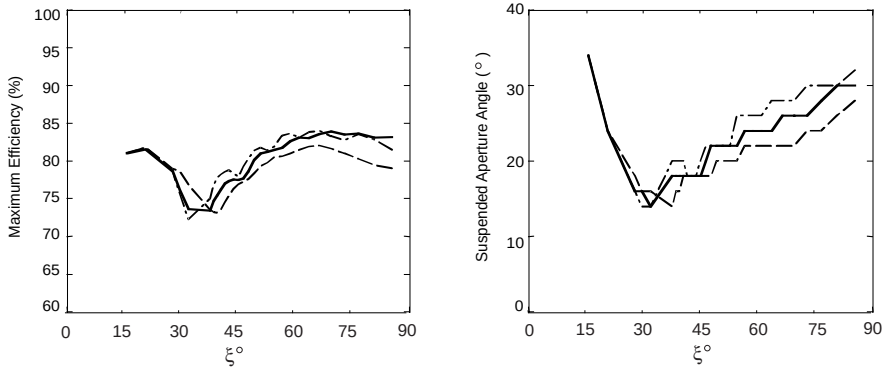

(a) (b)

Figure 11. Maximum reflector efficiency and the corresponding suspended angle versus the horn apex angle (- - - - Conical, —— profile 1 Gaussian, and −·− profile 2 Gaussian).

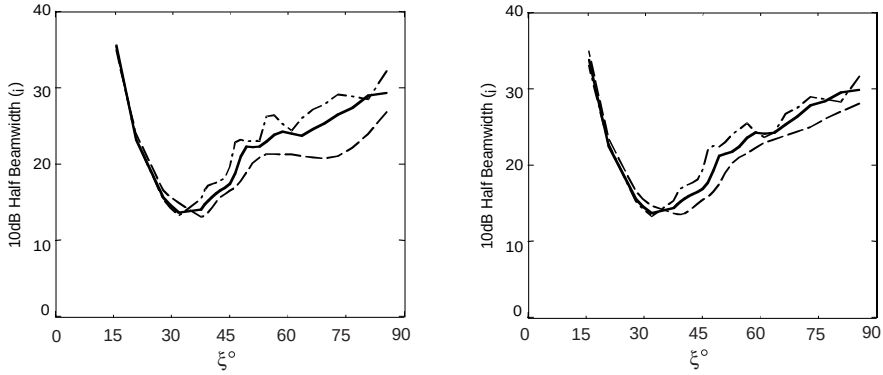

(a) (b)

Figure 12. 10 dB half beamwidth versus the horn apex angle, (a) E-plane, and (b) H-plane (- - - - Conical, —— profile 1 Gaussian, and −·− profile 2 Gaussian).

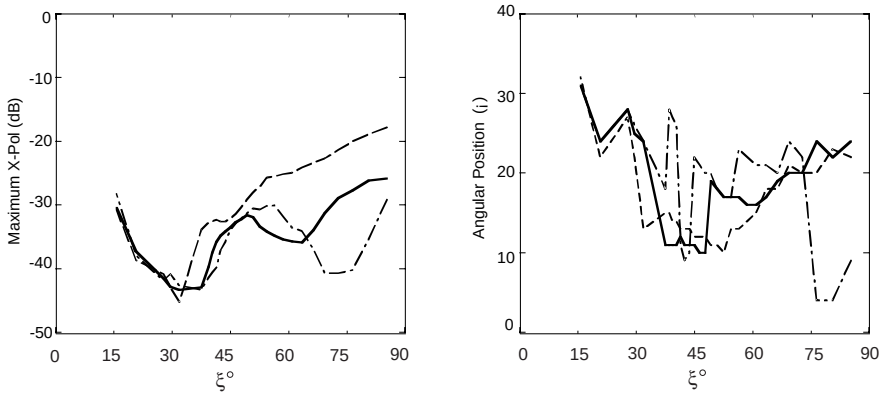

(a) (b)

Figure 13. Maximum cross polarization and its elevation position versus the horn apex angle. (---- Conical, —— profile 1 Gaussian, and −·− profile 2 Gaussian).

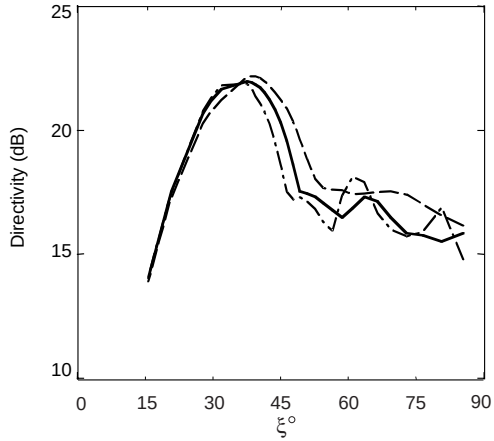

Figure 14. Directivity of the horn versus its apex angle (---- Conical, —— profile 1 Gaussian, and −·− profile 2 Gaussian).

between the horn and the waveguide. This is realized in the results obtained shown in Fig. 10 at larger apex angles. The graph in Fig. 11 shows that the two Gaussian profiled horn antennas provide higher efficiency as the horn apex angle increases. This high efficiency is almost 85%. Fig. 12 shows that the Gaussian profiled corrugated horns give more symmetrical radiation patterns compared to the conical corrugated horn. Fig. 13 shows that the two Gaussian profiled horns

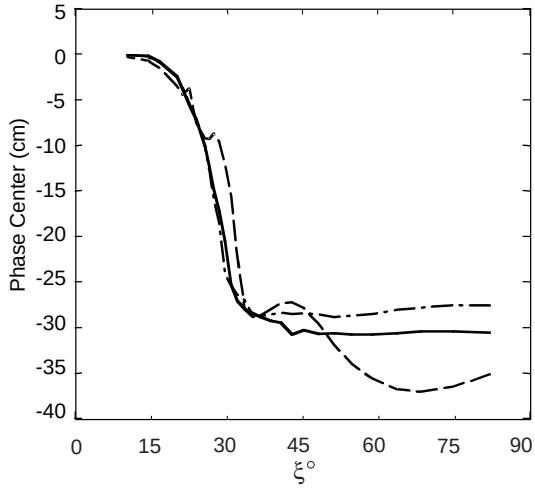

Figure 15. Phase center from the aperture of the horn versus the apex angle (---- Conical, —— profile 1 Gaussian, and −·− profile 2 Gaussian).

produce lower cross polarization levels compared to the conical horn. The corrugations made the directivity vary smoothly with the horn apex angle and the three horns have comparable directivities.

Next, the waveguide radii of the horn antennas are increased to 0.588λ to find out the influence of increased input mode mixtures to the performance of the horn antennas. The results obtained from Fig. 15 to Fig. 20 show that the performance of the conical corrugated horn antenna deteriorates as the waveguide radius increases in comparison with the monomode case of smaller waveguide radius. The corrugated horns with Gaussian profile maintain their performance.

Now, a sample of each corrugated horn is selected to show the radiation patterns for different frequencies. The horn samples are with $\mathbf{L} = 8\lambda$, $a_w = 0.4\lambda$ and $\mathbf{A} = 0.8$. The frequencies are varied from 7.5 GHz to 12.5 GHz. The results are tabulated in Fig. 21, which is distributed over four pages. It can be noted that the radiation patterns of the Gaussian profiled horns give lower cross polarization levels and much better pattern symmetry compared to the conical horn antenna within a wider frequency band. The performance of the conical horn improves gradually as the operating frequency is reduced. As for Gaussian profiled horns, very little change is noticed from the radiation patterns over the operating frequency range. The Gaussian profiled horn antennas give lower phase errors compared to conical horn

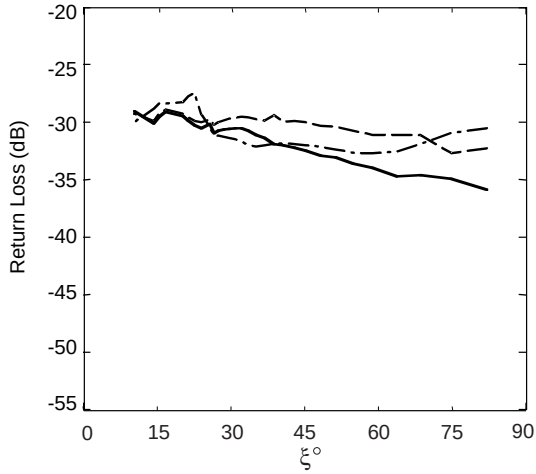

Figure 16. Return loss versus the horn apex angle (---- Conical, —— profile 1 Gaussian, and —·— profile 2 Gaussian).

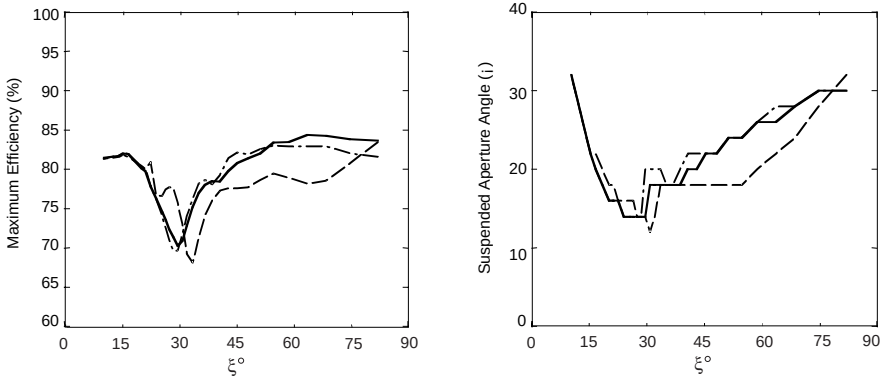

(a) (b)

Figure 17. Maximum reflector efficiency and the corresponding suspended angle versus the horn apex angle (---- Conical, —— profile 1 Gaussian, and —·— profile 2 Gaussian).

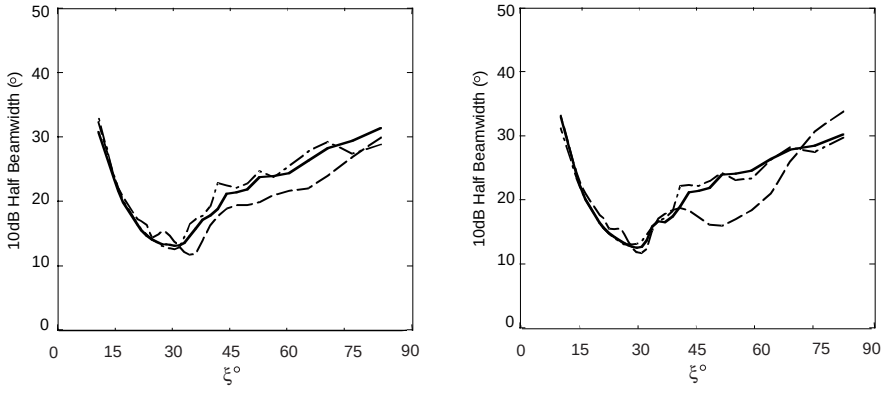

Figure 18. 10 dB half beamwidth versus the horn apex angle, (a) E-plane, and (b) H-plane (---- Conical, —— profile 1 Gaussian, and −·− profile 2 Gaussian).

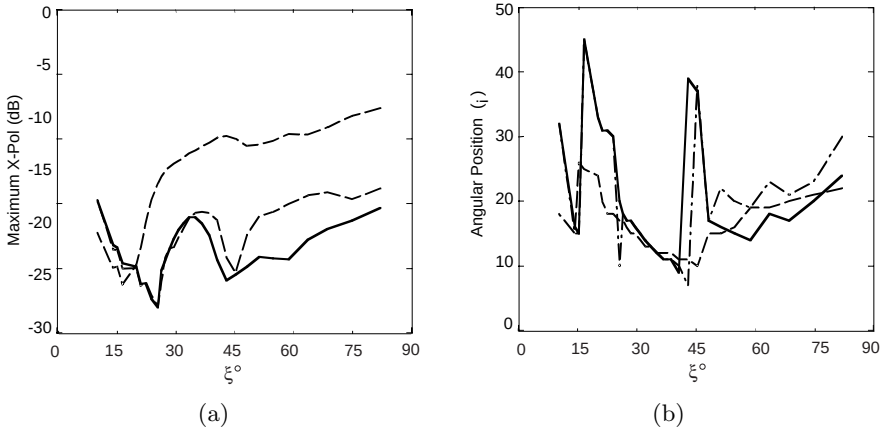

Figure 19. Maximum cross polarization and its elevation position versus the horn apex angle (---- Conical, —— profile 1 Gaussian, and −·− profile 2 Gaussian).

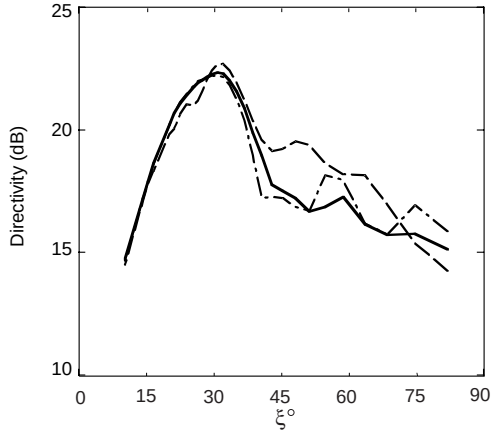

Figure 20. Directivity of the horn versus its apex angle (---- Conical, —— profile 1 Gaussian, and —·— profile 2 Gaussian).

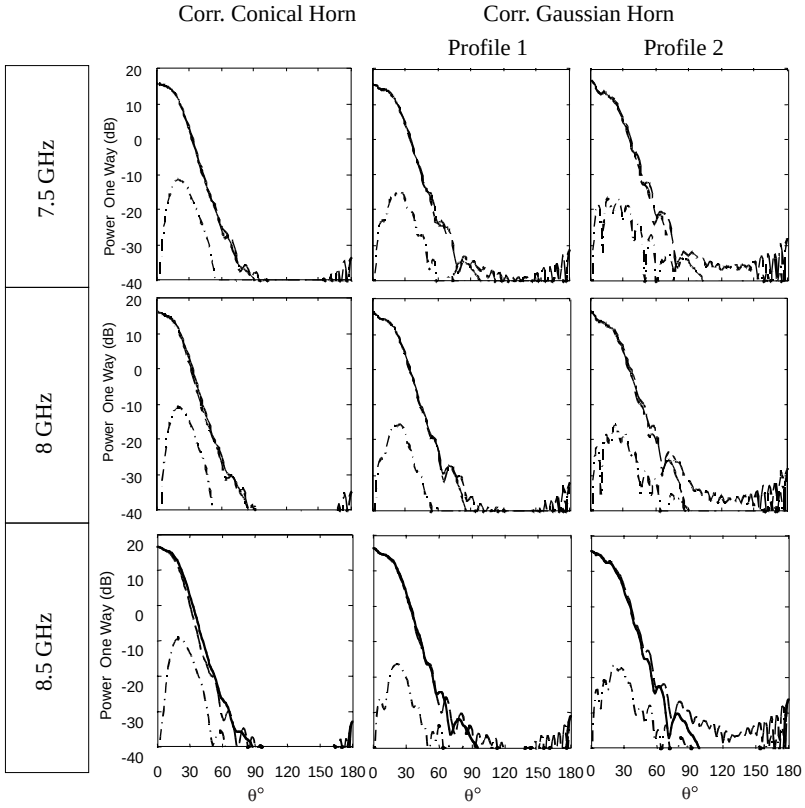

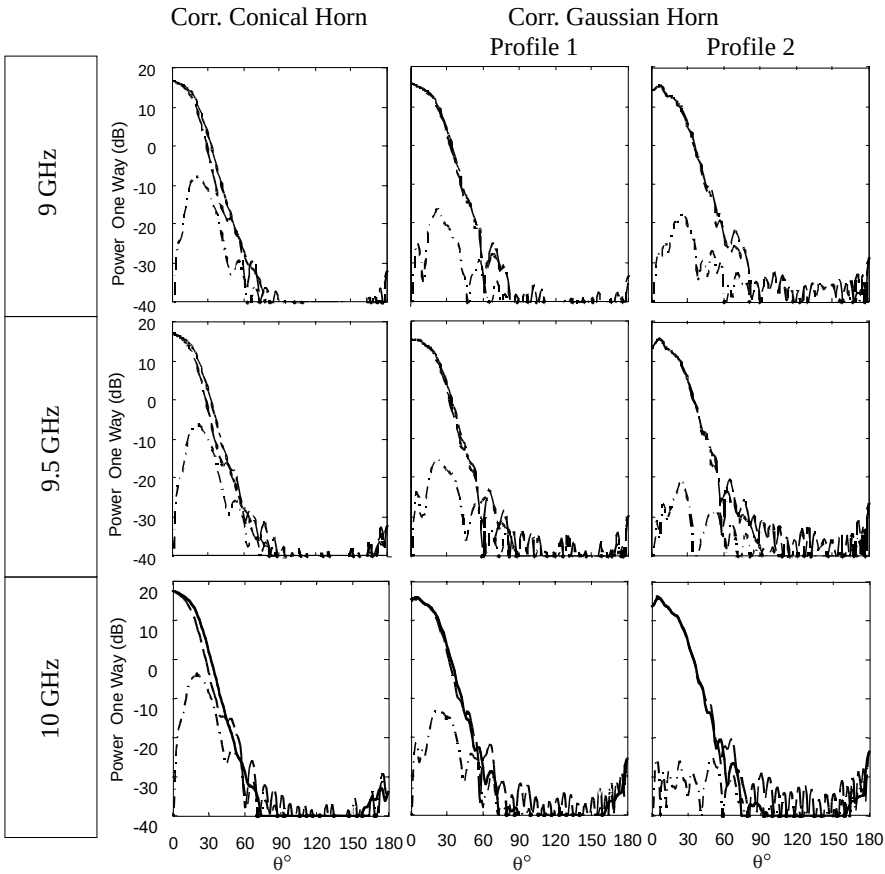

antenna. Since phase error is strongly frequency dependent, the conical horn antenna can only obtain an equal principle plane patterns over a narrow frequency range. Conical horn antennas therefore operate in a smaller bandwidth compared to the two Gaussian profiled horn antennas.

Finally, the results obtained for the horn antennas with $L = 8\lambda$ are compared with the results for the horns with $L = 4\lambda$ (omitted for brevity). We notice that the horn antennas at two different horn lengths present similar graph shapes. The Gaussian profiled horn antennas performing better than the conical horn antenna within their operating frequency range. The directivity and efficiency of the horn antennas increase as the length of the horn increases. Fig. 22 shows that after certain aperture diameter, the phase center moves to the waveguide aperture. To reach to this position, the horn apex angle needs to be larger for shorter horn antennas. The results also indicate

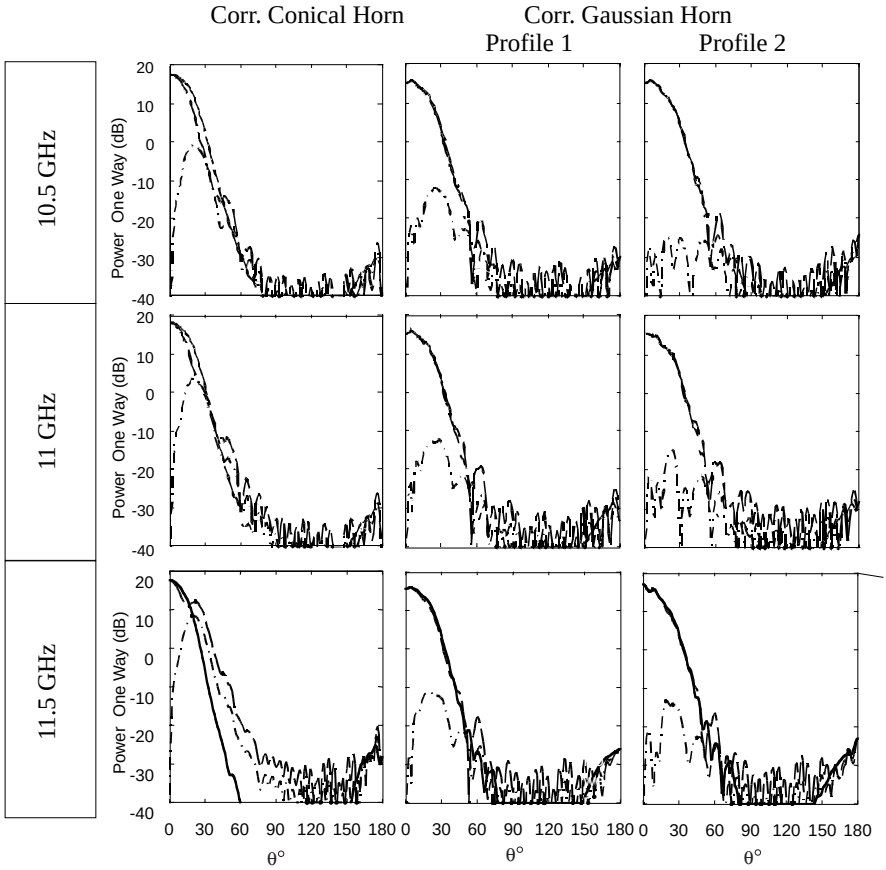

that although the aperture diameter of the Gaussian profiled horn is large, the aperture phase error remains small when compared to the phase error of the conical horn. Gaussian profiled horns have an overall smaller phase error compared to the conical horn because the smooth transition of the Gaussian profiled horn antennas produces more uniform amplitude and phase distribution that compensate for the spherical losses.

In the waveguide of the conical horn antenna, cylindrical waves with planar phase fronts are excited. The waves are then transformed to spherical wave phase fronts in the conical horn with a spherical cap at the aperture. Thus, when the horn apex angle increases, the aperture phase error increases causing a reduction in the horn directivity, as in Fig. 7. Also an increase in the return loss is noticed, as proven in Fig. 3. In contrast, the Gaussian profiled aperture horn antennas introduce a smooth transition to match the waveguide and

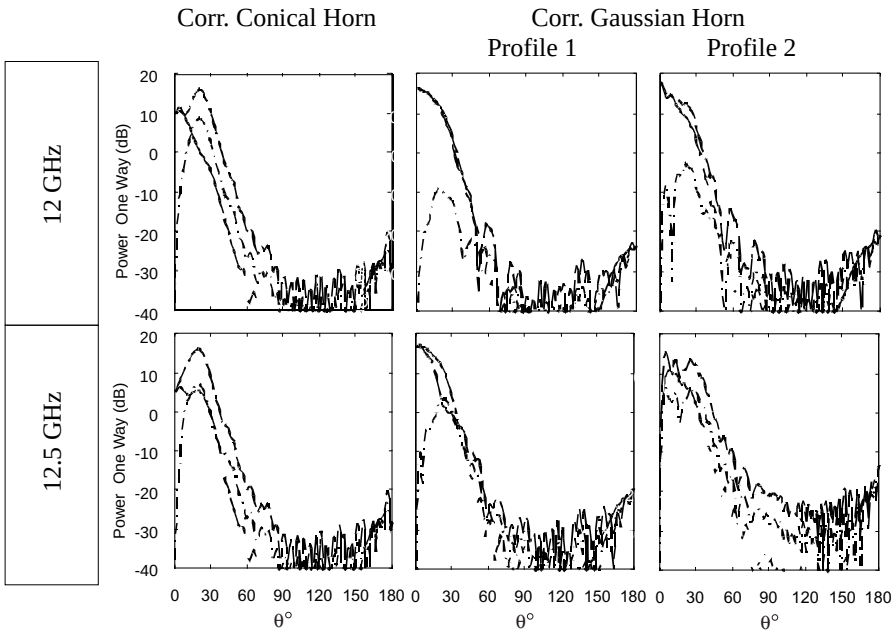

Figure 21. Radiation patterns of corrugated horn antennas at different frequencies with $a_w = 0.4\lambda$. (---- E-plane, —— H-plane, and $-\cdot-$ X-pol). (The figure is divided over the last 3 pages)

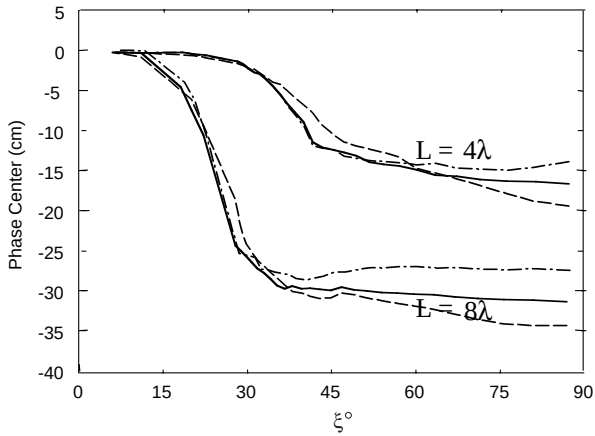

Figure 22. Phase center from aperture of the corrugated profile horn antennas (---- Conical Horn, —— profile 1 Gaussian horn, and $-\cdot-$ profile 2 Gaussian horn).

horn. This improves the matching between the waveguide and horn. This matching in the waveguide transforms the wave phase fronts from planar to spherical to planar again at the aperture of the horn. Planar phase fronts obtained from Gaussian profiled horns produce smaller aperture phase error compared with the non-planar phase front produced by the conical horns. Thus, the Gaussian profiled aperture horn antenna provides higher efficiency than the formally used conical horn antenna, as shown in Fig. 4. It is common knowledge that smooth-walled horn antennas operate in their dominant mode, TE_{11}, and have asymmetry radiation patterns. Thus, they do not give good radiation pattern and also do not show a significant advantage over one another, especially at smaller apex angles. Note that the above observations are only true with large apex angle.

6. CONCLUSION

In our studies regarding smooth-walled Gaussian profiled horns and smooth-walled conical horn antennas, the results have verified that the smooth transition between the waveguide and the aperture of the Gaussian profiled horns helps to improve the return loss and the efficiency when compared to the sudden transition between the waveguide and the aperture for the conical horn antenna. This explanation is supported by results obtained from the corrugated Gaussian profiled horns and the corrugated conical horn. The corrugated Gaussian profiled horns have better radiation characteristics when compared to the corrugated conical horn, such as lower return loss, higher efficiency (their efficiency obtained approaches 85% at larger output radius), wider beamwidth in the E-plane and H-plane, better symmetry of E-plane and H-plane and lower cross polarization levels. This make the corrugated Gaussian profiled horns more favorable to the corrugated conical horn. The smooth transition from the waveguide to the aperture of the Gaussian profiled horn antennas excites high purity hybrid modes that exhibit lower cross polarization and provide better radiation characteristics. The curvature of the Gaussian profiled horns allows matching of the waveguide to free space. This matching produces a circular wave with planer phase front that has negligible phase error.

Finally, the comparison between performances of the horns with aperture lengths equal to 8λ and 4λ indicates that the Gaussian profiled horn antennas continue to perform better than the conical horn antenna regardless of the length of the aperture. The increase of the length increases the directivity and efficiency of the horns, but does not dispute the fact that the Gaussian profiled horn antennas

perform better than the conical horn antenna within wider bandwidth. In general, one can conclude that the Gaussian profiled horn antennas perform better than the conical horn antenna due to its smoother transition between waveguide and aperture.

ACKNOWLEDGMENT

This work was supported by the National Science Foundation under Grant no. ECS-9810448.

REFERENCES

1. Love, A. W. (Editor), *Electromagnetic Horn Antennas,* IEEE Press, 1976.
2. Clarricoats, P. J. B. and A. D. Olver, *Corrugated Horns for Microwave Antennas,* IEE electromagnetics waves series 18, 1984.
3. Olver, A. D., P. J. B. Clarricoats, A. A. Kishk, and L. Shafai, *Microwave Horns and Feeds,* Chaps. 8 and 9, IEE electromagnetics waves series 39, 1994.
4. Spanish Patent P.9501922, "Horn antenna mode converter from waveguide modes to Gaussian structures," C. Del Río, R. Gonzola, M. Sorolla y M. Thumm, 25/09/1995.
5. Spanish Patent P.9601636, "Mode converter: From the TE11 monomode circular waveguide mode to the HE11 corrugated circular waveguide mode," C. Del Río, R. Gonzola, y M. Sorolla, 11/07/1996.
6. Del Río, C., R. Gonzola, and J. Teniente, "Gaussian profiled horn antennas," *7th International Symposium, Recent Advances in Microwave Technology Proceeding,* 199–202, 1999.
7. Del Río, C., R. Gonzola, and J. Teniente. "Very shorn and efficient feeder design from monomode waveguide," *IEEE-AP-S International Symposium,* 1997.
8. Del Río, C., R. Gonzola, and Y. M. Sorolla, "High purity Gaussian beam excitation by optimal orn antenna," *Proceedings of ISAP'96,* 1133–1136, Chiba, Japan, *IEEE-AP-S International Sym,* 1997.
9. Kishk, A. A., "Radiation and scattering from multi perfectly conducting axisymmetric surfaces using method of moments (BORPEC Version 2.01)," Software User's Guide, Sept 1999.
10. Ludwig, A. C., "The definition of cross-polarization," *IEEE Transactions on Antennas and Propagation,* Vol. AP-21, No. 1, 116–119, 1973.